Clays and Clay Minerals, Vol. 69, No. 2:289–298, 2021

CLOISITE 10A AS AN EFFECTIVE ANTIBACTERIAL AGENT IN POLYMER MATRICES: ROLE OF NANOSCALE ROUGHNESS AND INTERFACIAL INTERACTIONS

S. Snigdha[1,5], K. Nandakumar[1,4], T. Sabu[1,3], and E. K. Radhakrishnan[2,*]

[1] International and Inter-University Centre for Nanoscience and Nanotechnology, Mahatma Gandhi University, 686 560, Kottayam, Kerala, India
[2] School of Biosciences, Mahatma Gandhi University, 686 560, Kottayam, Kerala, India
[3] School of Chemical Sciences, Mahatma Gandhi University, 686 560, Kottayam, Kerala, India
[4] School of Pure and Applied Physics, Mahatma Gandhi University, 686 560, Kottayam, Kerala, India
[5] Department of Biotechnology, St. Joseph's College, Irinjalakuda, 680 121, Kerala, India

Abstract—Polymer–filler interactions play a major role in determining the antibacterial activity of organoclay in nanocomposites. The objective of the current study was to determine the effect of polymer type on the antibacterial properties of an organically modified clay – cloisite 10A (C10A) – using poly-ε-caprolactone (PCL) and poly-L-lactic acid (PLA) polymeric systems. Nanocomposite characterization using atomic force microscopy (AFM) showed an increase in roughness upon addition of the clay mineral, and X-ray diffraction (XRD) showed intercalation of the selected polymers into the interlayer spaces of the clay. Transmission electron microscopy (TEM) analysis supported the XRD findings. C10A in PCL thin films enhanced the bactericidal activity against *Staphylococcus aureus* when compared to the C10A in PLA. The observed change could be the result of pronounced levels of interaction between the filler and polymer matrix in the C10A-PLA nanocomposite when compared to C10A-PCL. The higher interaction levels could hinder the diffusion of bactericidal agents from the nanocomposite membranes. The present study provided insight into the nature of interaction between nanocomposite components and its impact on bioactivity, which can have applications in terms of generating engineered antibacterial materials.

Keywords—Antibacterial · Cloisite 10A · Intercalation · Modified clay · PCL · PLA · *Staphylococcus aureus*

INTRODUCTION

The addition of nanofillers improves the properties and performance of polymeric matrices; such materials are referred to as nanocomposites. Organoclays have been used extensively and researched as nanofillers due to their role in strengthening polymeric systems (Bower 1949; Pavlidou and Papaspyrides 2008). Native clay minerals usually must be functionalized in order to increase their compatibility with polymers (Usuki et al. 1993; 1995; Nguyen and Baird 2006). The addition of a clay mineral as a filler in polymer matrices has been demonstrated to increase the barrier properties, tensile strength, and temperature sensitivity of the polymer (Marras et al. 2008; Rhim et al. 2009).

Cloisite 10A (C10A) is a clay derived from montmorillonite (Mnt). Montmorillonite is a 2:1 phyllosilicate with the general formula $M_x(Al_{4-x}Mg_x)Si_8O_{20}(OH)_4$, where M is often a monovalent cation such as Na^+, which is exchangeable; x is the degree of isomorphic substitution between 0.5 and 1.3. C10A is produced from Mnt by first exchanging the Na^+ with quaternary dimethylbenzyl hydrogenated tallow ammonium ($((CH_3)_2\ N^+$(hydrogenated tallow) $(CH_2)(C_6H_6O_{12})$) (Zanetti et al. 2000; Manias et al. 2001) to render it compatible with the polymer (Merah and Mohamed 2019), then it is combined with and exfoliated in the selected polymer to form the clay-polymer nanocomposite. Organic cations are known to reduce the surface energy of the nanocomposite and provide better interaction between the clay mineral and the polymer matrix. The long chains of the organic moieties also aid in increasing the interlayer spacing of the Mnt. The increased spacing enhances clay–polymer interactions (Kornmann et al. 2001).

Clay-polymer nanocomposites are among the most widely used composites, and are preferred because of the ready availability of clay minerals and because they have been studied extensively over many decades (e.g. Pavlidou and Papaspyrides 2008); the earliest study was by Bower (1949). Biocompatible and environmentally friendly polymers such as poly-L-lactic acid (PLA) and poly-ε-caprolactone (PCL) have been used extensively for packaging and biomedical applications (Elias et al. 2016; Giannakas et al. 2016; Rodríguez-Tobías et al. 2016; Sun et al. 2016; Thomas et al. 2015). Hence, studies of the interaction between the clay mineral and these polymeric matrices in nanocomposites can determine their suitability for specific applications.

The intercalation of polymer chains into Mnt leading to expanded clay-polymer structures has been reported by several studies (e.g. Mehrotra and Giannelis 1989;

* E-mail address of corresponding author: radhakrishnanek@mgu.ac.in
DOI: 10.1007/s42860-021-00122-z

Vaia et al. 1993). The renewal of interest in clay-polymer nanocomposites led to great advancements in clay intercalation chemistry. Interfacial interactions of the polymer and organoclay platelets have been known to influence the ultimate properties of the polymer nanocomposites. Increased interactions have enhanced mechanical properties and fire resistance (Islam et al. 2017; Luo and Daniel 2003). The interfacial interactions between organoclay and polymer can lead to the formation of polymer crystals on the surface of clay tactoids resulting in a hybrid crystal layer. This hybrid layer promotes enhanced interactions between the clay and polymer (Ning et al. 2012). The changes in bioactive properties such as microbicidal efficiency with respect to polymer–filler interactions have not been studied in detail. Microbicidal quaternary ammonium salts within the organosilicate-polymer composites are to be investigated thoroughly. The functional groups in ion-exchanged organoclay confer the bactericidal properties and provide the basis for its increased demand in applications that require antibacterial surfaces. A detailed study into the effect of functional groups of clay minerals on polymer composite properties is important, therefore (Chandran et al. 2015; Sun et al. 2016).

Staphylococcus aureus is one of the most resilient microorganisms on earth. It is a leading cause of various opportunistic infections such as endocarditis, bacteremia, osteomyelitis, and skin and soft-tissue infections. It is also a leading cause of hospital-mediated and food-borne infections. *S. aureus* is a very formidable and unpredictable threat to humans due to its global distribution and ability to adapt rapidly to many environments. The persistence of these bacterial strains on every surface makes their eradication highly challenging (Turner et al. 2019). The distribution of infective MRSA (Methicillin-resistant *Staphylococcus aureus*) and the associated high mortality rate, despite the introduction of many antibiotics by the Food & Drug Administration (FDA, USA), call for the development of alternative multi-targeted antimicrobial materials (Casapao et al. 2014; Davis et al. 2015; Harkins et al. 2017).

In a previous study, the current authors worked on differential exhibition of antibacterial properties of the hydrophobic clay cloisite 30B in PCL and PLA (Babu et al. 2018). In continuation of this work, the properties of the hydrophilic cloisite C10A and its interactions with PLA and PCL were studied. The present study was carried out in order to observe and confirm the extent to which the microbicidal activity of C10A was affected by the matrix in which it was enclosed. The present study also aimed to corroborate the findings that were observed in the previous study (Babu et al. 2018) by using techniques such as AFM, FTIR, TEM, SEM, and antimicrobial assay. A further objective was to study the effectiveness of polymer–filler interactions, which, in the current (2020/2021) pandemic scenario, can have a profound effect on the development of antimicrobial materials (such as for use in biomedical and packaging applications) that help to prevent opportunistic bacterial infections.

MATERIALS AND METHODS

Sample Preparation

The solvent-casting technique was used to prepare nanocomposite thin films: 10 wt.% solutions of PCL (MW 70,000, Sigma Aldrich, St. Louis, Missouri, USA) and PLA (MW 20,000, Sigma Aldrich, St. Louis, Missouri, USA) were prepared in chloroform (Merck, Mumbai, India) and stirred mechanically overnight to ensure uniform mixing and dissolution of polymer chains. The neat PCL and PLA thin films thus prepared were labeled PC0 and PL0, respectively.

Solutions containing 5 wt.% C10A (Rockwood clay additives GmbH, Moosburg, Germany, CEC = 125 meq/100 g) in PCL and PLA were prepared as described above. The solutions containing organoclay were subjected to sonication in a bath sonicator for 30 min, to achieve uniform dispersion of the clay. These were cast uniformly onto glass Petri dishes and allowed to evaporate (Dottori et al. 2011). The nanocomposite thin films obtained were referred to as PC10 and PL10 for C10A-PCL and C10A-PLA respectively. These prepared membranes were oven dried for 12 h at 40 °C and used for various analyses.

Characterization Studies

Surface topography studies using atomic force microscopy (AFM). The surface topography of the prepared thin films was evaluated with the help of an atomic force microscope A-100 SPM (APE Research Nanotechnology, Basovizza, Trieste, Italy). The thin films were surface scanned in contact mode at a scan rate of 0.95–1.00 Hz. Mean surface average roughness (Ra) was evaluated using the built-in analysis software of the analytical instrument. The roughness profile was determined from average surface height deviations measured from the mean plane of the AFM images.

Diffraction studies. X-ray diffraction studies of the thin films (2 cm × 2 cm area; 2 mm thick) and organoclay (C10A) were carried out using a Bruker D8 Advance X-Ray Diffractometer (Hanau, Germany) with nickel-filtered CuKα radiation operating at 45 kV and 44 mA, with minimum step size of 0.001°2θ and Omega: 0.001°. All data were collected in the range 2–40°2θ with a scanning rate of 5°2θ/min. All the samples were examined in the dehydrated state (Babu et al. 2018).

High-resolution Imaging of Thin-film Samples Using HRTEM. Transmission electron microscopy was performed on the PL10 and PC10 samples. Ultrathin sections (~100 nm) of the thin film were obtained by means of an ultra-microtome fitted with a diamond knife. The PL10 samples were sectioned at room temperature, whereas the PC10 thin films were microtomed at –60°C which is the glass transition temperature of PCL. The micrographs of the samples were taken using a JEOL JEM 2100 transmission electron

https://doi.org/10.1007/s42860-021-00122-z Published online by Cambridge University Press

microscope (JEOL, Tokyo, Japan), with an accelerating voltage of 200 keV. *Image J* software was used to analyse the micrographs obtained.

Anti-staphylococcal activity of C10A polymer nanocomposites. Disk diffusion assay on Mueller Hinton Agar (MHA) plates was used to evaluate the antibacterial potential of the thin films (Rhim et al. 2009). *Staphylococcus aureus* MTCC96 strain was used as the test organism and cultured in Nutrient Broth (NB) for 18–24 h at 37ºC. Prepared MHA plates were swabbed with the test organism when their growth showed turbidity equivalent to 0.5 McFarland standard. The clay disks were prepared by immersing Whatman filter paper disks (4 mm in diameter) in a C10A suspension (5% clay in distilled water). These clay control disks were then air-dried and UV-sterilized. Nanocomposite thin-film disks (4 mm in diameter) were UV sterilized and placed on inoculated MHA plates. The plates were then incubated for 24 h at 37°C. The experiment was carried out in triplicate and the zone of inhibition around each disk was measured (mm).

Scanning electron microscopy imaging was also used to confirm the antibacterial activity against *S. aureus*. For this, the test strain was inoculated into 10 mL of NB in four separate vials. Into these vials, UV-sterilized thin film disks (4 mm in diameter) were introduced and incubated at 37 °C for 18–24 h. The thin-film disks were dehydrated further using increasing concentrations of ethanol (30, 50, 80, and 100% ethanol) for 2 min each. The treated thin-film samples were then dried and coated with gold and examined using a JEOL 6390 SEM JSM at 6 kV (Aggarwal et al. 2007).

Statistical analysis. Analysis of variance (ANOVA-One way) was performed on all experimental data.

RESULTS

Surface topography studies using AFM revealed thin, uniaxial fibril formations in the 3D topographic images (Fig. 1). The nanocomposite thin films did not exhibit fibrillary formations and clay particles could be detected in the matrix of the nanocomposite (Fig. 1). The Ra values were calculated from the roughness profile determined by AFM. The Ra of unmodified PCL and PLA film surfaces were 52.13 and 25.28 nm, respectively. PC10 showed a surface roughness (Ra) of 63.67 nm, whereas for PL10, Ra was 50.19 nm. Both clay-incorporated membranes showed evidence of increased surface roughness.

Diffraction Studies

The neat PLA film exhibited a reflection at 16.7°2θ and two other reflections, at 19.3 and 22.6°2θ (Fig. 2). The reflection at 16.7°2θ is ascribed to the (200) and/or (110) planes characteristic of orthorhombic crystals (Das et al. 2010). The reflections at 19.3 and 22.6°2θ correspond to the (203) and (105) lattice planes, respectively (Nam et al. 2003). The XRD profile of PCL had characteristic

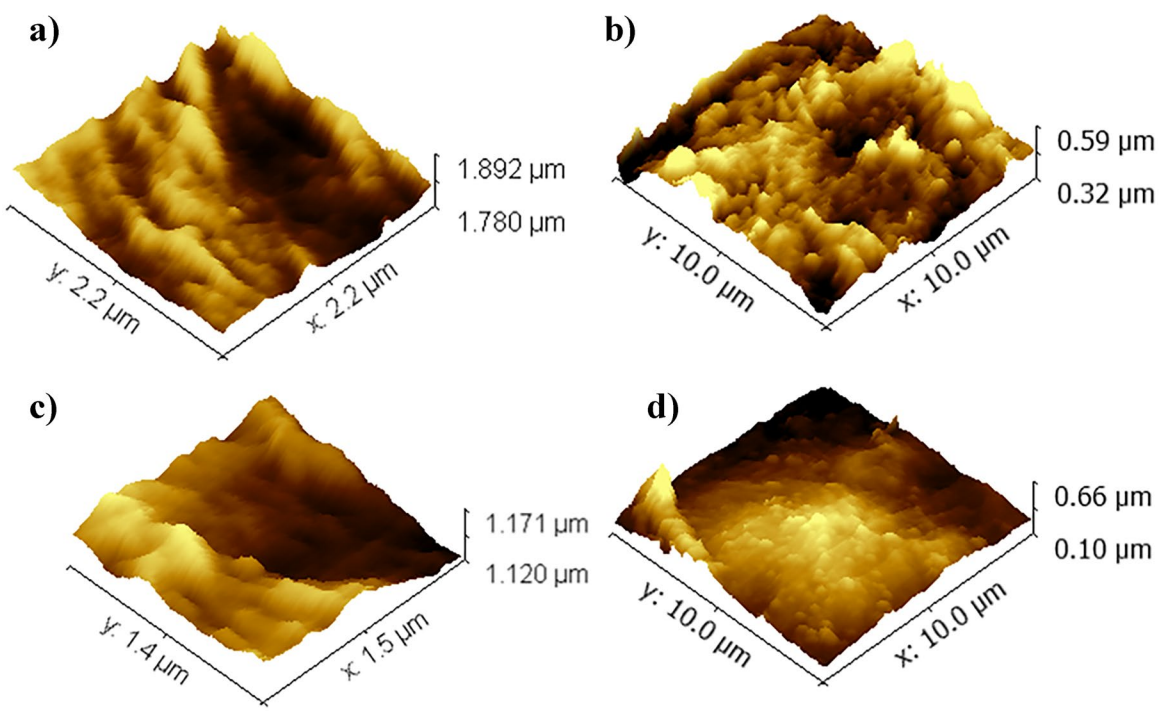

Fig. 1 Topographic AFM images of thin films of **a** PC0, **b** PC10, **c** PL0, and **d** PL10

https://doi.org/10.1007/s42860-021-00122-z Published online by Cambridge University Press

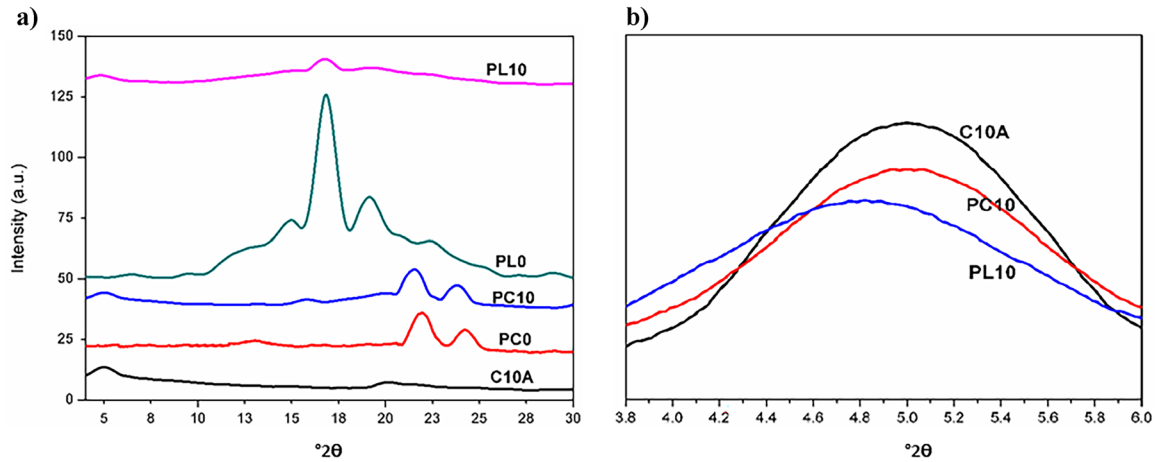

Fig. 2 XRD patterns of **a** prepared thin films and C10A and **b** magnified diffraction patterns of C10A, PL10, and PC10 showing a shifting of clay diffraction peaks to lower angles in the polymer matrix, especially in PL10

reflections at 21.4 and 23.8°2θ corresponding to the (110) and (200) planes of the semi-crystalline polymer (JCPDS number: 0–1431). The positions of PCL reflections in the nanocomposite were retained at 21.4 and 23.8°2θ (Fig. 2a). The XRD data of C10A showed a reflection at 5°2θ. The reflection by C10A in the PC10 thin film showed a slight shift to smaller diffraction angle, as it did in PL10 (4.8°2θ). The shift in 2θ values indicated the possible intercalation of the polymer into the interlayer space of the clays.

High-resolution Imaging of Thin-film Samples Using HRTEM

High-resolution TEM images corroborated the XRD data. The *d* values of the clay in the polymer matrix were measured using Image J software. The measurements were carried out at multiple positions on high-resolution images of the clay-polymer composites. The PL10 micrographs showed a larger degree of polymer intercalation than the PC10 nanocomposite. The PC10 exhibited a greater number of primary structures of C10A tactoids in the polymer matrix than in the PL10 matrix (Fig. 3a). The PL10 composite exhibited an average *d* value of 2.3 nm, consistent with the *d* values from XRD. The *d* values of PC10 averaged around 1.4 nm (Fig. 3b) (Das et al. 2010).

The TEM images also indicated that the organoclay had more exfoliation and slightly more intercalation in the PL10 matrix than in the PC10 matrix. Here, the PC10 matrix was marked by the existence of more primary structures of the organoclay with a *d* value of 1.4 nm (Fig. 3b). The TEM data provided visual confirmation of the data interpreted from the XRD pattern, therefore.

Anti-Staphylococcal Activity of C10A Polymer Nanocomposites

The antibacterial performance of C10A in PL10 and PC10 matrices was assessed (Fig. 4). The neat polymers had no antibacterial activity. A zone of inhibition of 12 mm was observed for the disks infused with C10A. Interestingly, PL10 and PC10 exhibited clearance zones of 8 and 16 mm, respectively (Fig. 4).

Upon incubation of the thin films in a nutrient broth culture and studying the SEM images (Fig. 5), the neat polymer thin films showed the presence of intact microbial colonies and the result was comparable to the disk-diffusion assay. The PC10 films showed microbial colonies with extensive cell-wall damage. In the case of PL10 films, isolated, intact microorganisms spread sparingly over the surface were observed, indicating the reduced adherence of the microbial cells to the membrane.

DISCUSSION

Polymer–filler interactions have been investigated widely (Chen 2004; Sorrentino et al. 2006), and from these, greater levels of interactions are considered to be desirable for enhanced performance of nanocomposites. The influence of these interactions on the expression of bioactive properties of the nanocomposite has not been investigated.

The present study, thus, aimed to investigate polymer–filler interactions and their effect on antibacterial activity of nanocomposite materials.

The morphological analysis of solvent-cast membranes developed in the study indicated the presence of thin, fibrillary structures in both neat thin films. The fibrillary structures probably occurred as a result of chain diffusion induced by crystallization of the polymer chain upon evaporation of the solvent (Cheng and Teoh 2004; Das et al. 2010). These fibrils were absent from clay-incorporated thin films; in that case, the organoclay may have interfered with the natural tendency of fibrillar crystallization of the polymer chains. The incorporation of clay into the polymer matrix may have induced interaction between the

https://doi.org/10.1007/s42860-021-00122-z Published online by Cambridge University Press

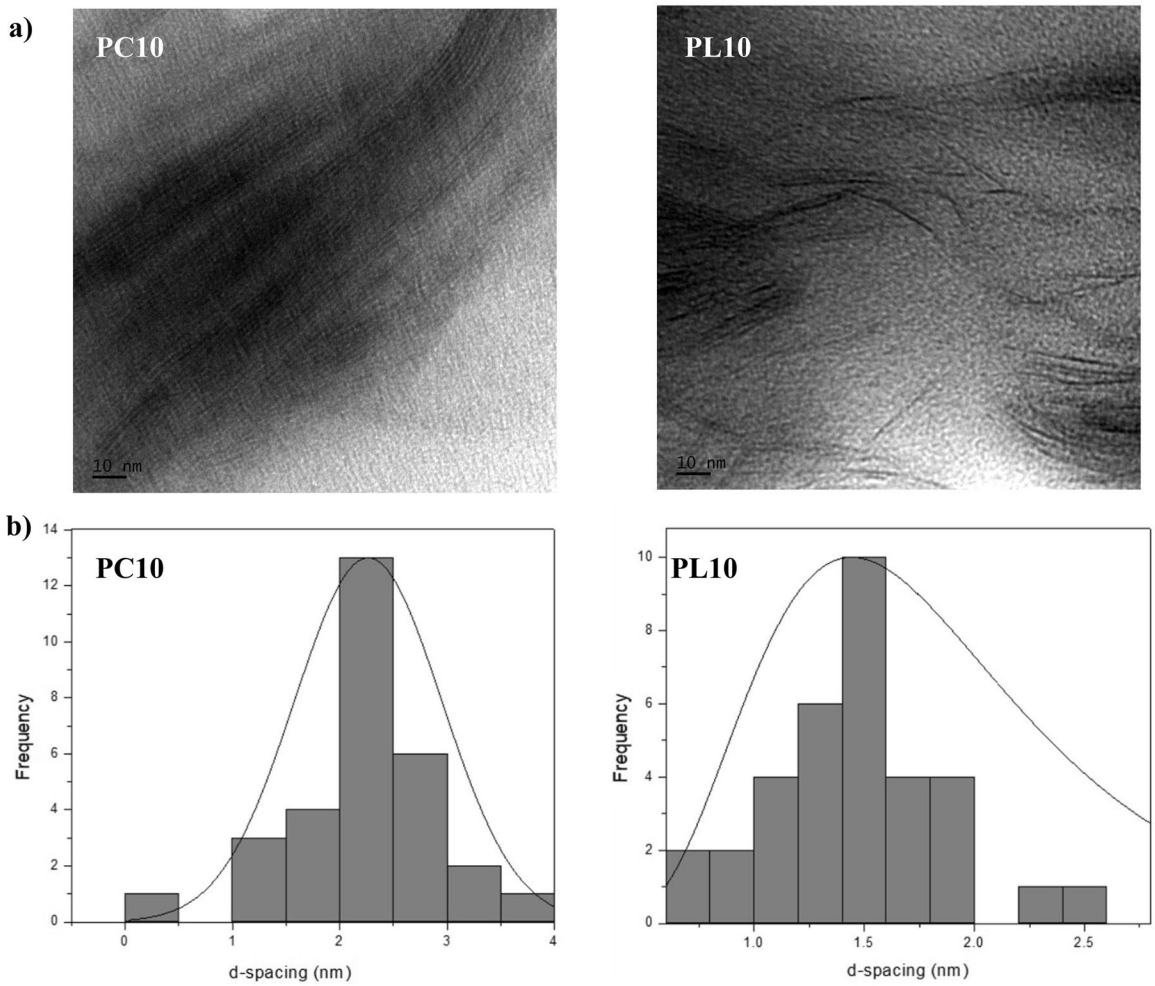

Fig. 3 TEM images of C10A-PLA nanocomposite showing a high level of intercalation in the C10A-PLA nanocomposite and the presence of primary organoclay structures in the C10A-PCL nanocomposite, and **b** *d*-spacing distribution for the polymer nanocomposites

components and thereby enhanced interfacial crystallization, hindering the typical crystallization tendencies of the polymer (Kim et al. 2014, 2016; Ning et al. 2012). Several studies have indicated that surface roughness decreases bacterial attachment on material surfaces (e.g. Kinnari et al. 2005; Rai et al. 2009). The nanoscale surface roughness is associated with high surface energy, resulting in decreased bacterial attachment (Zheng et al. 2012). Bacterial contact with the sharp edges of the nanowalls leading to membrane damage has also been demonstrated. In the present study, the addition of nanoclay resulted in the formation of various pointed projections (Fig. 1). In addition, the quaternary ammonium moieties released proved to be responsible for antibacterial activity (Beyth et al. 2006; Yudovin-Farber et al. 2010). The quaternary ammonium products released from the interlayer spaces in the clays also played a significant role in bactericidal action of the nanocomposite thin films (Hong and Rhim 2008; Maryan and Montazer 2015).

The XRD profile provided the structural insights into the polymer and clay–mineral interactions. The slight shift in organoclay reflections indicated polymer intercalation into the interlayer spaces of the clays. The polymer intercalation into C10A galleries was more pronounced in PLA than in PCL. The decreased intensity of the reflection of C10A in the nanocomposite suggests a highly disordered state of clay platelets in the nanocomposite. This disordered state is predominant in the PLA/C10A nanocomposite.

The XRD and TEM data also indicated better dispersion of C10A in a PLA matrix when compared to that of a PCL matrix. The chaotic arrangement of clay platelets in PLA may, therefore, have formed a barrier to the release of quaternary ammonium products, thereby leading to decreased antibacterial activity. This barrier effect may also have favored the quaternary ammonium moieties following a tortuous path through the nanocomposite matrix, thereby reducing significantly its bactericidal activity in the PLA nanocomposite (Li et al. 2011). The better dispersion

https://doi.org/10.1007/s42860-021-00122-z Published online by Cambridge University Press

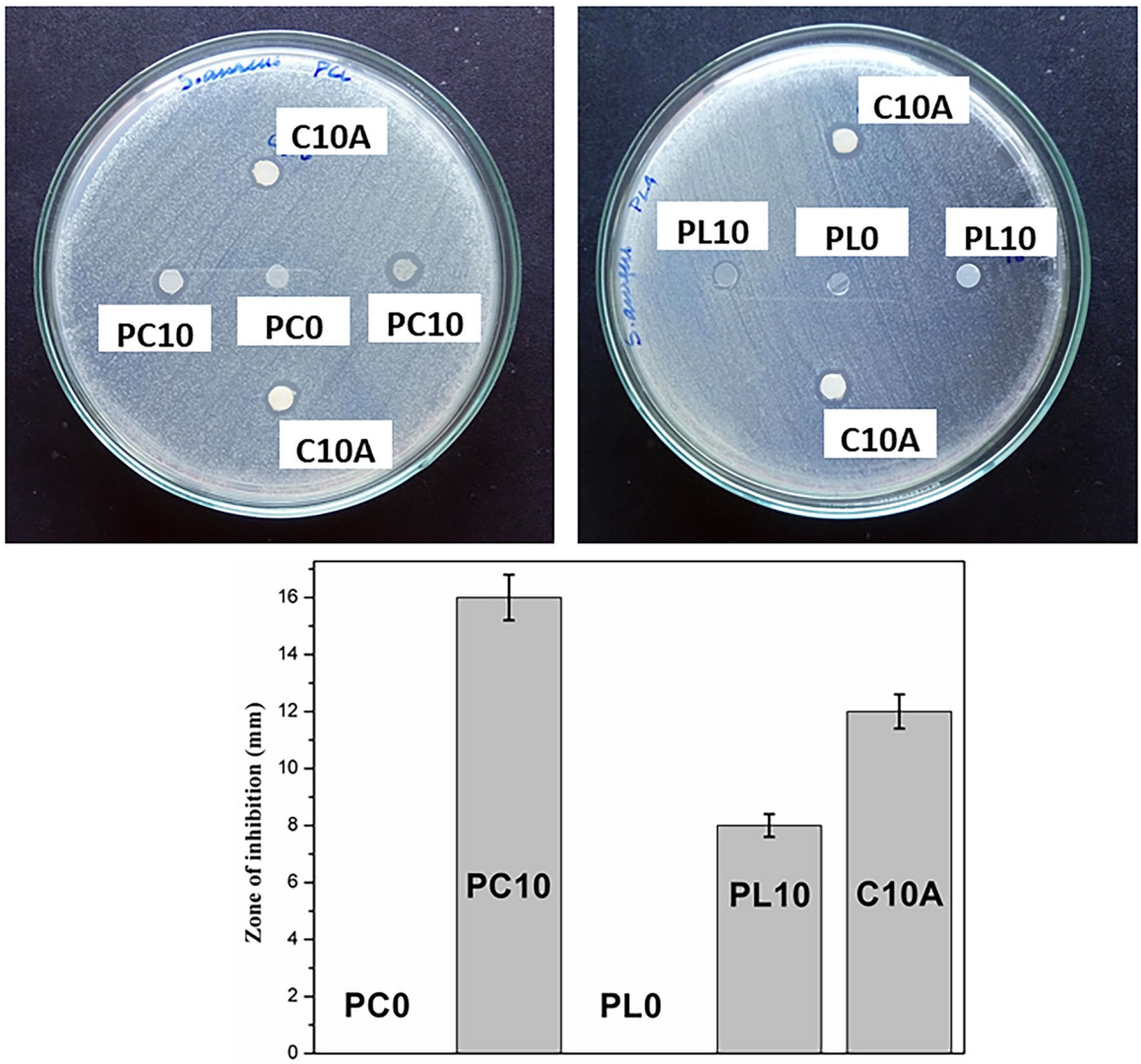

Fig. 4 Antimicrobial activity of the prepared thin films (PC0, PL0, PC10, PL10) against *Staphylococcus aureus*

of C10A in PLA was due to increased interaction between the polymer and clay owing to the presence of numerous hydroxyl groups in the organic modifier of C10A. The large surface area of C10A also contributed to the higher levels of interfacial interactions between the PLA and C10A (Chandran et al. 2015).

The increased crystallinity of PCL upon C10A addition could be due to the diffraction induced by the polymer layer formed over stacked organoclay induced by increased interfacial interactions between the components (Babu et al. 2016a). The decreased PLA crystallinity could be attributed to the highly disordered condition of organoclay in the PLA matrix, which disrupts the native crystallite structure formations characteristic of PLA. This was hampered also by the increased interfacial interactions between PLA and the clay (Fig. 6). The TEM images (Fig. 3) indicated the presence of native clay in their stacked forms in the PC10 films, whereas these highly ordered structures were noticeably absent from the PL10 nanocomposite (Chávez-Montes et al. 2016; Das et al. 2010). The XRD results presented here are, thus, consistent with the results of TEM analysis.

In the SEM images, the PC0 membrane showed the typical grape-shaped colonies of *S. aureus*, whereas the composite film PC10 depicted disrupted cell masses. The PL0 membrane had colonies characteristic of *S. aureus*, though the PL10 membrane had isolated, intact cells. The primary microbicidal activity observed here was due to alkyl ammonium moieties present in the organoclays. The cell walls of bacteria typically carry a net negative charge as a result of their carboxylate groups (Babu et al. 2018). The organoclay platelets are positively charged, which

https://doi.org/10.1007/s42860-021-00122-z Published online by Cambridge University Press

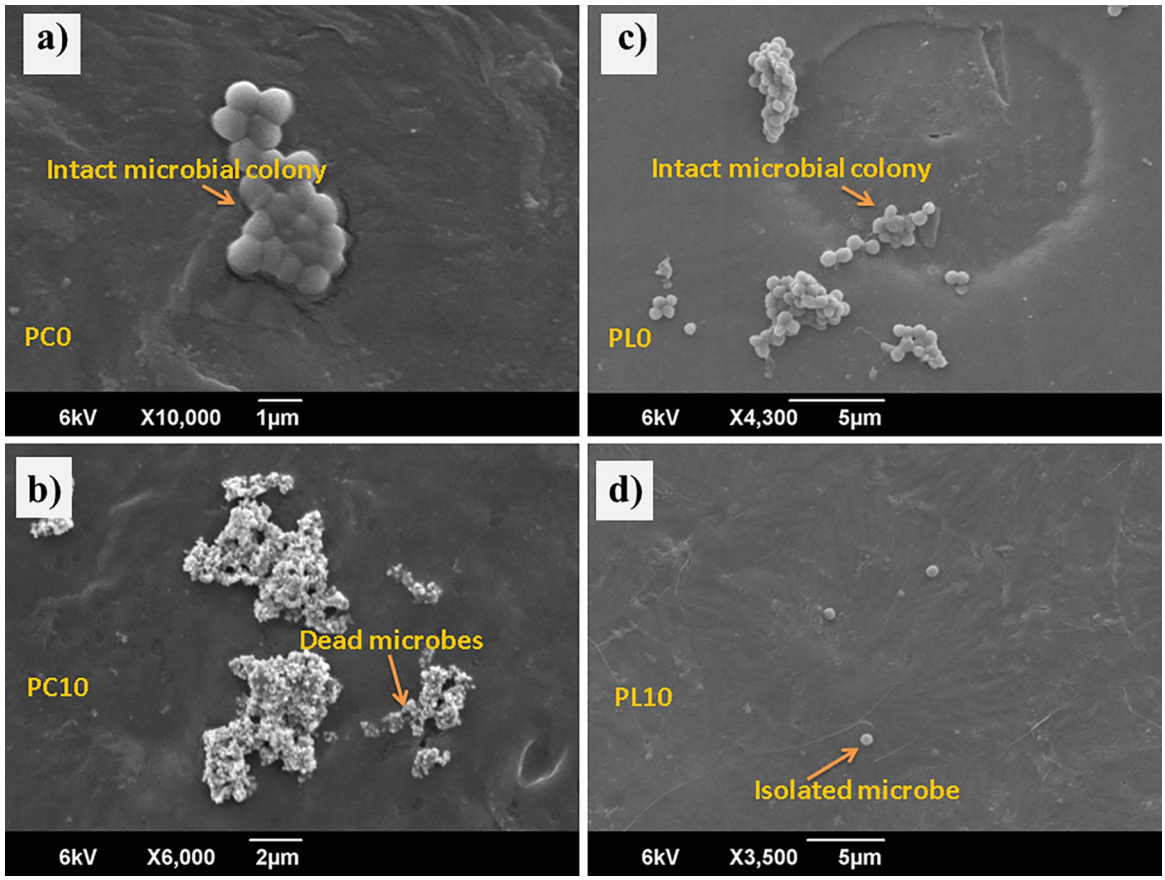

Fig. 5 SEM images of polymer thin films and composite thin films treated with *Staphylococcus aureus:* **a** PC0 showing an intact microbial colony, **b** PC10 showing dead bacteria with damaged cell walls, **c** PL0 showing intact microbial colonies, and **d** PL10 showing isolated microbes

attracts the bacterial cells through electrostatic interactions onto the surface of nanocomposites. The charge and hydrophobic interactions of the clay attract the bacteria onto the surface of the thin film, where the alkyl ammonium exerts its bactericidal actions (Babu et al. 2016b). The three main functional groups of PLA: ester, hydroxyl, and carboxyl groups, interact with the C10A through its hydroxyl groups. The presence of numerous hydroxyl moieties in both PLA and C10A favor greater interaction, thereby improving PLA crystallization (Chávez-Montes et al. 2016). The greater levels of interaction of PLA and C10A led to a slower release of the microbicidal moieties, which were manifested as reduced activity of C10A in PLA. The relatively lower levels of interactions between PCL and organoclay facilitated the effective release of the microbicidal moieties, resulting in increased activity (Fig. 6). The enhanced antibacterial activity exhibited by PC10 when compared to pristine organoclay is likely to be a cumulative effect of the diffusion of antibacterial moieties, surface roughness, and the hydrophobic and thermodynamic interactions between the thin film and the test organism (Babu et al. 2016b). In the case of PL10, the release of the antibacterial moieties was decreased, which resulted in less potent action compared to the PCL nanocomposite.

Results presented here highlight the significance of nanomaterials and polymer matrix selection in order to bring out the best in both materials, as revealed in a previous study using hydrophobic clay (Babu et al. 2018). The current work sheds light on the interactions between polymer and filler and their direct influence on antibacterial properties. This could aid in engineering materials with greater precision for packaging biomedical commodities where the use of antibiotics is expensive and potentially dangerous.

https://doi.org/10.1007/s42860-021-00122-z Published online by Cambridge University Press

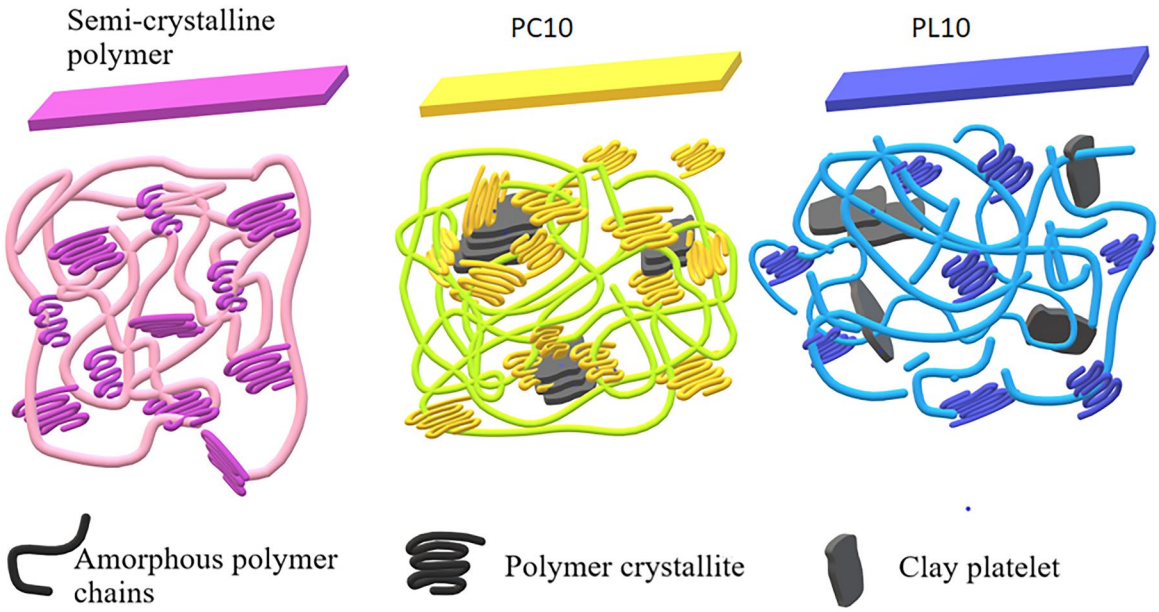

Fig. 6 Schematic representation of clay-polymer interactions in an unmodified semi-crystalline polymer, crystallites forming on the surface of the clay tactoids in PC10, and the highly disordered state of clay tactoids in the PLA matrix and the general decrease in crystallite formation in PL10

CONCLUSIONS

In the current study, a comparison of the effect of the microbicidal property of an organically modified clay within two polymer matrices was carried out. PLA and PCL were used to study the resultant antibacterial property as a function of their interactions with C10A and surface roughness. The XRD and TEM results revealed greater interactions between PLA and the organoclay when compared with PCL and organoclay. The increased interaction levels between the PLA and C10A resulted in slower release of the alkyl ammonium moieties and thereby decreased microbicidal activity. The reduced interactions between PCL and C10A, increased surface roughness, and physical interaction with the bacteria led to faster release and enhanced microbicidal activity of the nanocomposite. The PC10 composite showed significantly enhanced bactericidal action over the clay-PLA nanocomposite. The present study featured the importance of careful selection of materials in order to cater to the growing market for made-to-order nanocomposites.

ACKNOWLEDGMENTS

The authors are grateful for the facilities provided by the Department of Science and Technology of NANOMISSION (DST-Nanomission) and for the instrument facilities at the International and Inter-University Centre for Nanoscience and Nanotechnology, School of Chemical Sciences, School of Pure and Applied Physics, and School of Biosciences at the Mahatma Gandhi University, India.

Declarations

Conflict of Interest

The authors declare that they have no conflict of interest.

REFERENCES

Aggarwal, B. B., Surh, Y.-J., & Shishodia, S. (Eds.). (2007). *The Molecular Targets and Therapeutic Uses of Curcumin in Health and Disease*. Berlin: Advances in Experimental Medicine and Biology. Springer, Berlin.

Babu, S. S., Augustine, A., Kalarikkal, N., & Thomas, S. (2016a). Nylon 6, 12/Cloisite 30B electrospun nanocomposites for dental applications. *Journal of Siberian Federal University. Biology, 9*, 198.

Babu, S. S., Mathew, S., Kalarikkal, N., & Thomas, S. (2016b). Antimicrobial, antibiofilm, and microbial barrier properties of poly (ε-caprolactone)/cloisite 30B thin films. *3 Biotech, 6*, 249.

Babu, S. S., Kalarikkal, N., Thomas, S., & Radhakrishnan, E. (2018). Enhanced antimicrobial performance of cloisite 30B/poly (ε-caprolactone) over cloisite 30B/poly (L-lactic acid) as evidenced by structural features. *Applied Clay Science, 153,* 198–204.

Beyth, N., Yudovin-Farber, I., Bahir, R., Domb, A. J., & Weiss, E. I. (2006). Antibacterial activity of dental composites containing quaternary ammonium polyethylenimine nanoparticles against *Streptococcus mutans*. *Biomaterials, 27*, 3995–4002.

https://doi.org/10.1007/s42860-021-00122-z Published online by Cambridge University Press

Bower, C. (1949). Studies on the form and availability of organic soil phosphorous. *IOWA Agriculture Experiment Station Research Bulletin*, 362–339.

Casapao, A. M., Davis, S. L., Barr, V. O., Klinker, K. P., Goff, D. A., Barber, K. E., & 5 others. (2014). Large retrospective evaluation of the effectiveness and safety of ceftaroline fosamil therapy. *Antimicrobial Agents and Chemotherapy, 58*, 2541–2546.

Chandran, N., Chandran, S., Maria, H. J., & Thomas, S. (2015). Compatibilizing action and localization of clay in a polypropylene/natural rubber (PP/NR) blend. *RSC Advances, 5*, 86265–86273. https://doi.org/10.1039/c5ra14352g

Chávez-Montes, W. M., González-Sánchez, G., & Flores-Gallardo, S. G. (2016). Poly-lactide/exfoliated C30B interactions and influence on thermo-mechanical properties due to artificial weathering. *Polymers, 8*, 154.

Chen, B. (2004). Polymer–clay nanocomposites: an overview with emphasis on interaction mechanisms. *British Ceramic Transactions, 103*, 241–249.

Cheng, Z., & Teoh, S. H. (2004). Surface modification of ultra thin poly (ε-caprolactone) films using acrylic acid and collagen. *Biomaterials, 25*, 1991–2001. https://doi.org/10.1016/j.biomaterials.2003.08.038

Das, K., Ray, D., & Banerjee, I. (2010). Crystalline morphology of PLA/clay nanocomposite films and its correlation with other properties. *Journal of Applied Polymer Science, 118*, 143–151. https://doi.org/10.1002/app.32345

Davis, J. S., Sud, A., O'Sullivan, M. V., Robinson, J. O., Ferguson, P. E., & Foo, H., et al. (2015). Combination of vancomycin and β-lactam therapy for methicillin-resistant Staphylococcus aureus bacteremia: a pilot multicenter randomized controlled trial. *Clinical Infectious Diseases, 62,* 173–180.

Dottori, M., Armentano, I., Fortunati, E., & Kenny, J. (2011). Production and properties of solvent-cast poly (ε-caprolactone) composites with carbon nanostructures. *Journal of Applied Polymer Science, 119*, 3544–3552.

Elias, E., Chandran, N., Souza, F. G., & Thomas, S. (2016). Segmental dynamics, morphology and thermomechanical properties of electrospun poly (ε-caprolactone) nanofibers in the presence of an interacting filler. *RSC Advances, 6*, 21376–21386.

Giannakas, A., Vlacha, M., Salmas, C., Leontiou, A., Katapodis, P., Stamatis, H., Barkoula, N.-M., & Ladavos, A. (2016). Preparation, characterization, mechanical, barrier and antimicrobial properties of chitosan/PVOH/clay nanocomposites. *Carbohydrate Polymers, 140*, 408–415.

Harkins, C. P., Pichon, B., Doumith, M., Parkhill, J., Westh, H., Tomasz, A., & 4 others. (2017). Methicillin-resistant *Staphylococcus aureus* emerged long before the introduction of methicillin into clinical practice. *Genome Biology, 18*, 130.

Hong, S.-I., & Rhim, J.-W. (2008). Antimicrobial activity of organically modified nano-clays. *Journal of Nanoscience and Nanotechnology, 8*, 5818–5824.

Islam, M. S., Azmee, N., Ashaari, Z., AdibAiman, A., Rasyid, A., & Islam, K. H. N. (2017) Properties of wood polymer nanocomposites impregnated with ST-co-EDA/Nanoclay. *Macromolecular Symposia, 371*, 125–128. Wiley Online Library.

Kim, I. Y., Park, S., Kim, H., Park, S., Ruoff, R. S., & Hwang, S. J. (2014). Strongly-coupled freestanding hybrid films of graphene and layered titanate nanosheets: An effective way to tailor the physicochemical and antibacterial properties of graphene film. *Advanced Functional Materials, 24*, 2288–2294.

Kim, I. Y., Lee, J. M., Hwang, E.-H., Pei, Y.-R., Jin, W.-B., Choy, J.-H., & Hwang, S.-J. (2016). Water-floating nanohybrid films of layered titanate–graphene for sanitization of algae without secondary pollution. *RSC Advances, 6*, 98528–98535.

Kinnari, T. J., Peltonen, L. I., Kuusela, P., Kivilahti, J., Könönen, M., & Jero, J. (2005). Bacterial adherence to titanium surface coated with human serum albumin. *Otology & Neurotology, 26*, 380–384.

Kornmann, X., Lindberg, H., & Berglund, L. A. (2001). Synthesis of epoxy–clay nanocomposites: influence of the nature of the clay on structure. *Polymer, 42*, 1303–1310.

Li, Q., Yoon, J.-S., & Chen, G.-X. (2011). Thermal and biodegradable properties of poly(l-lactide)/poly(ε-caprolactone) compounded with functionalized organoclay. *Journal of Polymers and the Environment, 19*, 59–68. https://doi.org/10.1007/s10924-010-0256-2

Luo, J.-J., & Daniel, I. M. (2003). Characterization and modeling of mechanical behavior of polymer/clay nanocomposites. *Composites Science and Technology, 63*, 1607–1616.

Manias, E., Touny, A., Wu, L., Strawhecker, K., Lu, B., & Chung, T. (2001). Polypropylene/montmorillonite nanocomposites. Review of the synthetic routes and materials properties. *Chemistry of Materials, 13*, 3516–3523.

Marras, S. I., Kladi, K. P., Tsivintzelis, I., Zuburtikudis, I., & Panayiotou, C. (2008). Biodegradable polymer nanocomposites: the role of nanoclays on the thermomechanical characteristics and the electrospun fibrous structure. *Acta Biomaterialia, 4*, 756–765. https://doi.org/10.1016/j.actbio.2007.12.005

Maryan, A. S., & Montazer, M. (2015). Natural and organomontmorillonite as antibacterial nanoclays for cotton garment. *Journal of Industrial and Engineering Chemistry, 22*, 164–170.

Mehrotra, V. & Giannelis, E. (1989). Conducting molecular multilayers: intercalation of conjugated polymers in layered media. *MRS Online Proceedings Library Archive, 171*.

Merah, N. & Mohamed, O. (2019). Nanoclay and water uptake effects on mechanical properties of unsaturated polyester. *Journal of Nanomaterials,* article 8130419.

Nam, J. Y., Sinha Ray, S., & Okamoto, M. (2003). Crystallization behavior and morphology of biodegradable polylactide/layered silicate nanocomposite. *Macromolecules, 36*, 7126–7131.

Nguyen, Q. T., & Baird, D. G. (2006). Preparation of polymer–clay nanocomposites and their properties. *Advances in Polymer Technology, 25*, 270–285. https://doi.org/10.1002/adv.20079

Ning, N., Fu, S., Zhang, W., Chen, F., Wang, K., Deng, H., Zhang, Q., & Fu, Q. (2012). Realizing the enhancement of interfacial interaction in semicrystalline polymer/filler composites via interfacial crystallization. *Progress in Polymer Science, 37*, 1425–1455.

Pavlidou, S., & Papaspyrides, C. D. (2008). A review on polymer–layered silicate nanocomposites. *Progress in Polymer Science, 33*, 1119–1198. https://doi.org/10.1016/j.progpolymsci.2008.07.008

Rai, M., Yadav, A., & Gade, A. (2009). Silver nanoparticles as a new generation of antimicrobials. *Biotechnology Advances, 27*, 76–83.

Rhim, J.-W., Hong, S.-I., & Ha, C.-S. (2009). Tensile, water vapor barrier and antimicrobial properties of PLA/nanoclay composite films. *LWT-Food Science and Technology, 42*, 612–617.

Rodríguez-Tobías, H., Morales, G., & Grande, D. (2016). Improvement of mechanical properties and antibacterial activity of electrospun poly (D, L-lactide)-based mats by incorporation of ZnO-*graft*-poly (D, L-lactide) nanoparticles. *Materials Chemistry and Physics, 182*, 324–331.

Sorrentino, A., Tortora, M., & Vittoria, V. (2006). Diffusion behavior in polymer–clay nanocomposites. *Journal of Polymer Science Part B: Polymer Physics, 44*, 265–274.

Sun, Z., Fan, C., Tang, X., Zhao, J., Song, Y., Shao, Z., & Xu, L. (2016). Characterization and antibacterial properties of porous fibers containing silver ions. *Applied Surface Science, 387*, 828–838.

Thomas, R., Soumya, K., Mathew, J., & Radhakrishnan, E. (2015). Electrospun polycaprolactone membrane incorporated with biosynthesized silver nanoparticles as effective wound dressing material. *Applied Biochemistry and Biotechnology, 176*, 2213–2224.

Turner, N. A., Sharma-Kuinkel, B. K., Maskarinec, S. A., Eichenberger, E. M., Shah, P. P., Carugati, M., Holland, T. L., & Fowler, V. G., Jr. (2019). Methicillin-resistant *Staphylococcus aureus*: an overview of basic and clinical research. *Nature Reviews Microbiology, 17*, 203–218.

Usuki, A., Kojima, Y., Kawasumi, M., Okada, A., Fukushima, Y., Kurauchi, T., & Kamigaito, O. (1993). Synthesis of nylon 6-clay hybrid. *Journal of Materials Research, 8*, 1179–1184.

Usuki, A., Koiwai, A., Kojima, Y., Kawasumi, M., Okada, A., Kurauchi, T., & Kamigaito, O. (1995). Interaction of nylon 6-clay surface and mechanical properties of nylon 6-clay hybrid. *Journal of Applied Polymer Science, 55*, 119–123.

Vaia, R. A., Ishii, H., & Giannelis, E. P. (1993). Synthesis and properties of two-dimensional nanostructures by direct intercalation of polymer melts in layered silicates. *Chemistry of Materials, 5*, 1694–1696.

Yudovin-Farber, I., Golenser, J., Beyth, N., Weiss, E. I., & Domb, A. J. (2010). Quaternary ammonium polyethyleneimine: antibacterial activity. *Journal of Nanomaterials*. https://doi.org/10.1155/2010/826343

Zanetti, M., Lomakin, S., & Camino, G. (2000). Polymer layered silicate nanocomposites. *Macromolecular Materials and Engineering, 279*, 1–9.

Zheng, Y., Li, J., Liu, X., & Sun, J. (2012). Antimicrobial and osteogenic effect of Ag-implanted titanium with a nanostructured surface. *International Journal of Nanomedicine, 7*, 875.

(Received 2 November 2019; revised 9 March 2021; AE: Jin-Ho Choy)